# Detecting Precise Iris Boundaries by Circular Shortest Path Method

Ivan Matveev[1] and Ivan Simonenko[2]

[1]Computing Centre of Russian Academy of Sciences,
Vavilov str., 40, Moscow, 119333, Russia
[2]Moscow Institute of Physics and Technology,
Institutskii per., 9, Dolgoprudny, Moscow Region, 141700, Russia

**Abstract.** Modified circular shortest path detection method is applied for refining pupil and iris boundaries using given approximate pupil and iris circles. Brightness gradient direction is employed to choose image pixels, which may belong to pupil or iris boundary. Using initial approximate circles allows the method to work in a narrow ring, which contains only single circular contour. Under these conditions the method allows to correctly handle almost all images used for iris recognition tasks and appears to be more precise than human expert in marking the pupil border. The method was tested with public domain iris databases, containing more than 80000 images totally.

## 1 Introduction

Iris recognition is one of main biometric identification technologies. Detecting iris borders in image is an important part of this method. Iris pattern in image is represented as a ring enclosed between two approximately circular and approximately concentric contours: inner border, which is an iris-pupil boundary, and outer border, which is iris-sclera boundary. Both boundaries are approximated by circles with good precision, however there are applications demanding more precise shape detection and description [1]. This particularly concerns inner (i.e. pupil) boundary. As a rule, human pupil is close to circle in shape, however in most cases it is not an ideal circle and has irregular deviations with relative magnitude around 5-10% [2]. Thus, a problem appears to detect a contour, which has approximately circular shape and encloses dark region (pupil) in relatively brighter background. Apparently, iris can be detected as a dark circular region in a background of sclera, in case there are no or small occlusions by eyelashes and eyelids. Problem of detecting shapes modelled by circles and ellipses (i.e. regular shapes) have attracted much attention and many methods are developed. Rich variability of methods applied to determining iris boundaries is reviewed in [3, 4]. Much less attention is attracted to tracking the boundaries to their irregular (although close to circle) shape that may allow better recognition performance. Many researchers limit themselves to just an iteration of same detection algorithm [5, 6] or to applying same detection method in different scale under multi-scale image processing scheme [7, 8]. Special methods for refinement of the boundaries, which track roundish but irregular shapes with good

Matveev I. and Simonenko I..
Detecting Precise Iris Boundaries by Circular Shortest Path Method.
DOI: 10.5220/0004394501010108
In *Proceedings of the 4th International Workshop on Image Mining. Theory and Applications* (IMTA-4-2013), pages 101-108
ISBN: 978-989-8565-50-1

precision and tolerate noise were developed to much less extent. The authors could find that only one approach of active contours was specially targeted and tested with the task of iris border refinement [9–11]. Here a method of circular shortest path proposed in [12] is modified and applied to the problem of refining pupil and iris borders.

## 2 Circular Shortest Path Algorithm

There are plenty of methods performing detection of shortest path in images. Specific feature of the CSP approach among them is that it starts from an a-priory detected point that is claimed to be an approximate contour center (or at least is lying inside the contour). In the refinement task stated here initial data for the method are even more detailed: center position and radius of approximating circle are given. Since the contour passes round a given point it is reasonable to perform a polar transformation with the pole in this point, which simplifies both representation and calculations. (Indeed, polar transformation is a very common issue in iris image processing.) Polar transformation renders a ring shape to a rectangle. This rectangle can be positioned so as to have its top side being a circle enclosing the proposed contour (enough big circle should be taken), and bottom side is to be enough small circle inside the contour. Then left side and right side both correspond to a coordinate origin line, let it be $OX$ half-axis. The radial coordinate of polar system is transformed to abscissa of the rectangle and angle coordinate becomes ordinate. Image in $OXY$ domain is transformed to $O\rho\phi$ domain and is also represented as a rectangular raster. Define the size of the raster as $W * H$ pixels. Call it *polar representation rectangle*, see. Figure1.

After the polar transformation circular path location task is rendered to a problem of detecting optimal path between left and right sides of rectangle, under the condition that terminal points at the sides have same vertical coordinate. Since contour is close to circle in shape and pole of the polar transform is inside it, the polar representation of contour is univalent, i.e. only one radius of contour corresponds to each angle value, and the contour can be expressed in terms of function $\rho(\phi)$, $\phi \in [0; 2\pi]$, $\rho(0) = \rho(2\pi)$. Further, assuming that pole of transformation is not very close to the contour line (in other words, is near the center of the contour), one can state that derivative of radius by angle is limited: $d\rho/d\phi \leqslant 1$. In raster polar representation rectangle of size $W * H$ this function becomes a discrete sequence $\{\rho_n\}$ (or accounting for both coordinates $\{(n, \rho_n)\}$), $n \in [0, W-1]$, $\rho_n \in [0; H-1]$. Limitation to derivative becomes $|\rho_{n+1} - \rho_n| \leqslant 1$. Condition to equal value at ends becomes $|\rho_{W-1} - \rho_0| \leqslant 1$. Thus the contour is represented as a chain of points in rectangular raster, each column of the raster contains one and only one contour point, the points in adjacent columns belong to same or adjacent rows, the first and last points also belong to same or adjacent rows. Hereinafter this chain of points is called *path* $S = \{\rho_n\}_{n=0}^{W-1}$. Figure2 illustrates the possible paths of a contour, if tracked from left to right. A path from point with coordinates $(\phi; \rho) = (2; 3)$ can go to points $(3; 2) - (3; 4)$, from point $(5; 1)$ - into points $(6; 1)$ and $(6; 2)$, and if staring point is $(1; 2)$ ending points can be $(8; 1) - (8; 3)$.

Introduce the cost of transition between points $(n, \rho')$ and $(n+1, \rho'')$ in adjacent columns in polar representation. Define it as $C((n, \rho'), (n+1, \rho''))$, or shorter $C_n(\rho', \rho'')$. It is composed from "inner" and "outer" parts: $C(\rho', \rho'') = C^{(I)}(\rho', \rho'') +$

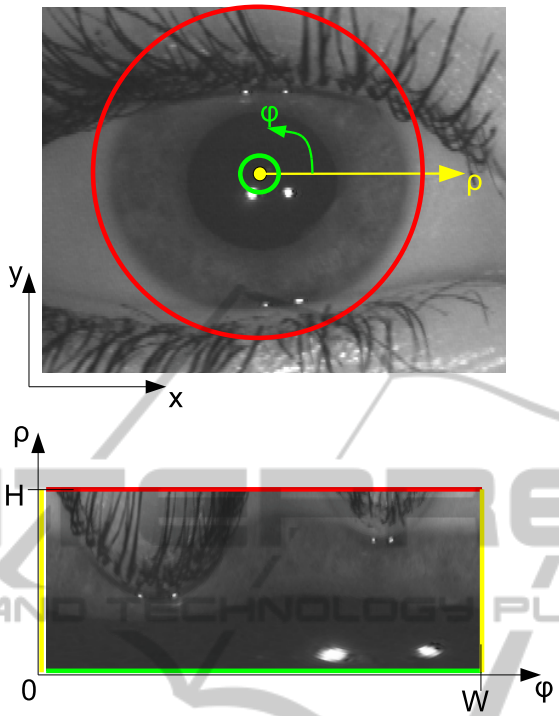


**Fig. 1.** Sample of polar transform applied to an iris image.

| | | | | | | | |
|---|---|---|---|---|---|---|---|
| | | | | | | | |
| | | (3,4) | | | | | |
| | (2,3) | (3,3) | | | | | (8,3) |
| (1,2) | | (3,2) | | | (6,2) | | (8,2) |
| | | | | (5,1) | (6,1) | | (8,1) |

**Fig. 2.** Possible contour paths in case of limited derivative $d\rho/d\phi \leqslant 1$.

$C^{(O)}(\rho', \rho'')$. Inner part conditions the shape of the contour and favours straight horizontal lines (which are circles in original $OXY$ domain):

$$C_n^{(I)}(\rho', \rho'') = \begin{cases} 0\ , & \rho' = \rho'' \\ T_1\ , & |\rho' - \rho''| = 1 \\ \infty\ , & otherwise \end{cases}$$

The constant $T_1 > 0$ is the parameter which determines a "force" compelling the contour to be a straight line in polar representation (i.e. circle with center in given

pole in original image). The value of $T_1$ depends on parameters of polar transform, namely from the scale of polar representation. While inner part depends on contour shape only, and does not depend on image, outer part is estimated from image characteristics and binds the contour to image. The outer part is the cost of passing through point $(n, \rho')$ determined from local image characteristics in the point, and does not depend on contour shape: $C_n^{(O)}(\rho', \rho'') = w((n, \rho'))$. For a given path $S = \{\rho_n\}_{n=0}^{W-1}$ total cost is the sum of all transitions between adjacent points in the path: $C(S) = C((0, \rho_0), (W, \rho_W)) = \sum_{n=0}^{W-1} C_n(\rho_n, \rho_{n+1})$. The optimal contour is the sequence minimizing the whole cost: $S^* = arg\min_S C(S)$. This discrete optimization problem may be solved by some known method, for instance, greedy algorithm as proposed in [12].

## 3 Application to Pupil Boundary Refinement

Application of CSP method to the problem of iris boundaries detection has specific issues. First, it is obvious that there are two circular contours in the image of an eye: pupil-iris boundary and iris-sclera boundary. Sometimes there is a contour of ophthalmic lens also. This makes it difficult to apply CSP method to initial detection of these borders, since detected contour can be any of these two and there is no perfect way of discriminating these two cases. This application was treated in [13]. So, feasible task for CSP method is refinement of already detected pupil and iris borders. Under this condition initial approximate locations of both iris boundaries is known. Thus the algorithm can run for a narrow ring containing the target boundary, rather than for the whole image. For a narrow polar representation rectangle with $H < 30$ a straightforward exhaustive search is faster than other elaborated algorithms.

The exhaustive search of optimal circular path is performed recursively as a set of steps. Each step involves a column of the polar representation raster (points with same value of $\phi$). The cost of passing from a point $(0, \rho')$, in the first (left) column to the point $(n, \rho'')$, in current column: $C((0, \rho'), (n, \rho'')) \equiv C_{(n)}(\rho', \rho'')$. Since both $\rho'$ and $\rho''$ range in $[1, H]$, it is necessary to calculate $H^2$ values $C_{(n)}$. They are calculated recursively starting from $C_{(1)}(\rho', \rho'') = 1/\delta(\rho', \rho'')$. For each next column the cost of arriving to a point in it is a minimal sum of cost of arriving to some point $\rho'''$ in the previous column and the cost of transition between adjacent columns:

$$C_{(n+1)}(\rho', \rho'') = \min_{\rho'''}(C_{(n)}(\rho', \rho''') + C_n(\rho''', \rho'')) =$$

$$= \min \begin{Bmatrix} C_{(n)}(\rho'), \rho'') + w(n, \rho'') \ , \\ C_{(n)}(\rho'), \rho'' + 1) + w(n, \rho'' + 1) + T_1 \ , \\ C_{(n)}(\rho'), \rho'' - 1) + w(n, \rho'' - 1) + T_1 \ , \end{Bmatrix}$$

The incoming path for each point in the column (i.e. which of the three sums gave minimum) is recorded. At the final step (which has number $W+1$) $H^2$ values $C_{(W+1)}(\rho', \rho'')$ are obtained. Only values with $\rho' = \rho''$ correspond to closed contours. So the cost of optimal closed contour is $\min_\rho C_{(W+1)}(\rho, \rho)$ and it starts and ends at $\rho^*_{W+1} \equiv \rho^*_0 =$

$arg\min_{\rho} C_{(W+1)}(\rho,\rho)$. From the detected radius $\rho^*_{W+1}$ contour is tracked back easily from the recorded incoming paths.

Now consider the outer cost of transition via point $C^{(O)}(\phi,\rho) = w(\phi,\rho)$. From the task formulation it is clear that $w(\phi,\rho)$ function should be constructed so as to be small in the points corresponding to the contour and big in other points. Contour points have strong brightness gradient value, thus points with small gradient should be rejected. This is done in the source image by checking the condition $\|\mathbf{g}\| > T_2$ in each image pixel and selecting only pixels, which satisfy this condition as possible contour points. Here $\mathbf{g}$ is is brightness gradient vector and $T_2$ is a threshold. The value of $T_2$ is selected so as to suppress false gradients occurring due to image noise. If $3*3$ Sobel mask is used for gradient calculation the treshold can be set $T_2 = 6\sqrt{2}\max\{\sigma, 2\}$, where $\sigma$ is the brightness standard deviation caused by noise.

Next task-specific feature is that both pupil and iris are dark regions in brighter background, hence brightness gradients are directed outwards of the contour, and the angle between gradient in the point and radius-vector to this point from the center of the contour is enough small. This condition can be set as: $arccos(\frac{\mathbf{x}\cdot\mathbf{g}}{\|\mathbf{x}\|\,\|\mathbf{g}\|}) < T_3$. The value of threshold $T_3$ depends on the quality of the center detection algorithm, treated as an average (or maximum, or percentile) ratio of the distance $D$ between detected center and true center to the radius $R$ of the contour. It is calculated as $T_3 = \arcsin(D/R)$. Figure3 shows the points of an image from Figure1, satisfying both of the above conditions. The cost of transition is set to zero for these points, and is set to $T_1$ for all other points.

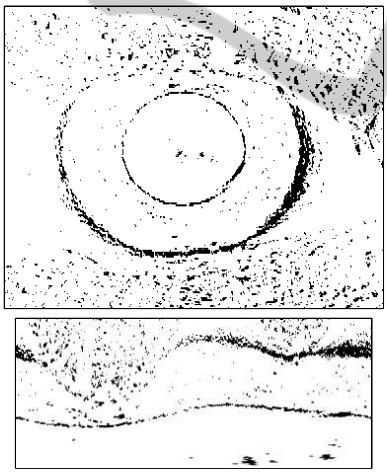

**Fig. 3.** Sample of gradient map with direction condition imposed and its polar transform.

With these modifications CSP method was applied to the refinement of iris boundaries

## 4 Experiments

Tests of CSP performance were done with the following iris image databases from public domain: UBIRIS.v1 [14], CASIA-IrisV3 [15], ND-IRIS [16]. Eye images were

processed by human expert who indicated pupil and iris borders with most likely approximating circles. Thus each image was attributed with center positions and radii of pupil and iris circles. These data (call it *expert marking*) were then considered as "ground-truth" and were used for method verification. Unfortunately, there is no simple way to obtain refined border contours, that can be treated as "ground-truth". Human operator can manually mark quite a small share of huge image databases with such contours. This task is much more tedious and error-prone than marking circles.

So, direct tests of comparing refined borders to some "ground-truth" data and testing the quality of refinement method are not possible. Indirect methods were used instead. Refined borders were "simplified" back to circle, which has center in the point of mass center of the area, enclosed to the refined border. Radius of simplified circle was set to equate areas enclosed in this circle and in refined border. Call this simplified representation of refined border *refined circle*. Although again circle, refined one does not match the original approximation, and it can be a better approximation somehow.

Two approaches were used to compare original and refined circles. First approach is direct matching against expert marking, to estimate which kind of detection is more precise. Images from all three databases were used [14–16]. Three ways were used to supply initially detected pupils and irises. First, expert marking data itself were spoiled with random noise to simulate improper detection. Second, Masek's algorithm [17] was used. Third, an approximate method of detection by circular brightness gradient projections [18] was employed. Mean square deviations of pupil center position and radius from expert marking were calculated for all three ways for original and refined circles.



**Table 1.** Error in pupil detection by various methods.

| Method | Average error of pupil radius detection in three databases, pixels | | | Average error of pupil center position in three databases, pixels | | |
|---|---|---|---|---|---|---|
| | UBI | NDIRIS | CASIA | UBI | NDIRIS | CASIA |
| Spoiled expert | 8.16 | 8.16 | 8.16 | 5.77 | 5.77 | 5.77 |
| Masek | 4.65 | 7.23 | 5.15 | 3.24 | 5.59 | 3.67 |
| Matveev | 7.78 | 6.34 | 5.81 | 5.13 | 4.27 | 4.11 |
| Spoiled expert, refined | 5.59 | 2.52 | 1.86 | 3.26 | 1.63 | 1.53 |
| Masek, refined | 4.07 | 2.41 | 1.58 | 2.88 | 2.07 | 1.14 |
| Matveev, refined | 4.89 | 2.09 | 1.45 | 3.51 | 1.52 | 1.09 |

CSP refinement makes improvement in precision of initial detection, although it is not effective for highly noisy images like UBIRIS.v1.

Second approach to estimate the quality and usability of refinement is judging by the "final characteristic", that is precision of iris recognition. The value of equal probability of recognition errors of first and second kind (*equal error rate, EER*) was chosen as such characteristic. CASIA Iris-Lamp database [15] was used for tests, which contains 16213 images of 819 eyes of 411 subjects. The following steps were performed here. Templates were created from images of database by the algorithm [9]. For its work the algorithm uses circular approximations of pupil and iris in each image. At first, pure expert marking was used for this purpose. The set of obtained templates was matched against itself and the EER value was estimated. For original expert marking its value is

EER=0.752%. Then expert marking of pupils was refined by the proposed method, and same operations of template generation, matching and EER evaluation were done, with resulting EER=0.390%.

So, the refinement of pupil by circular shortest path method appears to reduce the recognition error. This can be explained by the imprecise marking of human expert.

## 5 Conclusions

Location of iris borders with high precision is an important task in automatic iris biometry. Though much attention is paid to iris border location in general, only few researchers tried developing special methods for iris border refinement after their initial detection. The authors have treated this aspect of iris border location problem with the help of circular shortest path optimization method. The CSP detection algorithm was modified to fit the peculiar properties of the task. The results of experiments show that refinement of pupil-iris boundary by CSP may be a useful addition to general scheme of iris border location.



## References

1. ISO/IEC 19794-6:2005 Information technology – Biometric data interchange formats – Part 6: Iris image data, 2005.
2. Kansky, J.J.: Clinical Ophthalmology: a Systematic Approach, Elsevier, London, 2003.
3. Bowyer, K., Hollingsworth, K., and Flynn, P.: Image understanding for iris biometrics: A survey // Computer Vision and Image Understanding. 2008. P.281–307.
4. Bowyer, K., Hollingsworth, K., and Flynn, P.: A survey of iris biometrics research: 2008-2010 // Handbook of Iris Recognition, Mark Burge and Kevin W. Bowyer, editors. Springer. 2012.
5. He, Z., Tan, T., Sun, Z., and Qiu, X. Toward accurate and fast iris segmentation for iris biometrics. In IEEE PAMI. 2009. V.31. P.1670–1684.
6. Maenpaa, T. An iterative algorithm for fast iris detection. In Int. Workshop on Biometric Recognition Systems. Beijing. China.. 2005. P.127.
7. Nabti, M., Ghouti, L., and Bouridane, A. An effective and fast iris recognition system based on a combined multiscale feature extraction technique. In Pattern Recognition. 2008. V.41. P.868–879.
8. Pan, L., Xie, M., and Ma, Z. Iris localization based on multiresolution analysis. In Proc. 19th Intern. Conf. Pattern Recognition. Tampa, Florida, USA.. 2008. P.1–4.
9. Daugman, J.: New methods in iris recognition // IEEE Trans. on Systems, Man and Cybernetics. Part B: Cybernetics. 2007. V.37. P.1167-1175.
10. Ross, A., Shah, S.: Segmenting non-ideal iris using geodesic active contours // Biometrics Symposium: Special Session on Research at the Biometric Consortium Conf. Baltimore. USA, 2006. P.16.
11. Koh, J., Govindaraju, V., Chaudhary, V.: A robust iris localization method using an active contour model and hough transform // 20th Int. Conf. on Pattern Recognition. Istanbul. Turkey. 2010. P.2852-2856.
12. Sun, C., Pallottino, S.: Circular shortest path in images // Pattern Recognition. 2003. V.36. N.3. P.709-719.

13. Matveev, I.A.: Circular Shortest Path as a Method of Detection and Refinement of Iris Borders in Eye Image // Journal of Computer and Systems Sciences International. 2011. V.50. N.5. P.778-784.
14. Proenca, H., Alexandre, L.A.: UBIRIS: A noisy iris image database // 13th Intern. Conf. on Image Analysis and Processing. V.3617. Cagliari, Italy: Springer, 2005. P.970-977.
15. Chinese academy of sciences institute of automation (CASIA), CASIA Iris image database http://www.cbsr.ia.ac.cn/IrisDatabase.htm, 2005.
16. Phillips, P.J., Scruggs, W.T., O'Toole, A.J. et al. Frvt2006 and ice2006 large-scale experimental results // IEEE PAMI. 2010. V.32. .5. P.831-846.
17. Masek, L.: Recognition of human iris patterns for biometric identification. http://www.csse.uwa.edu.au/ pk/studentprojects/libor, 2003.
18. Matveev, I.A.: Detection of Iris in Image By Interrelated Maxima of Brightness Gradient Projections // Applied and Computational Mathematics, 2010, V.9, No.2, pp.252-257.